TOWARDS CERTIFIABLE ADVERSARIAL SAMPLE DETECTION

Ilia Shumailov *
University of Cambridge
ilia.shumailov@cl.cam.ac.uk

Yiren Zhao *
University of Cambridge
yiren.zhao@cl.cam.ac.uk

Robert Mullins
University of Cambridge
robert.mullins@cl.cam.ac.uk

Ross Anderson
University of Cambridge
ross.anderson@cl.cam.ac.uk

February 21, 2020

ABSTRACT

Convolutional Neural Networks (CNNs) are deployed in more and more classification systems, but adversarial samples can be maliciously crafted to trick them, and are becoming a real threat. There have been various proposals to improve CNNs' adversarial robustness but these all suffer performance penalties or other limitations. In this paper, we provide a new approach in the form of a certifiable adversarial detection scheme, the Certifiable Taboo Trap (CTT). The system can provide certifiable guarantees of detection of adversarial inputs for certain l_∞ sizes on a reasonable assumption, namely that the training data have the same distribution as the test data. We develop and evaluate several versions of CTT with a range of defense capabilities, training overheads and certifiability on adversarial samples. Against adversaries with various l_p norms, CTT outperforms existing defense methods that focus purely on improving network robustness. We show that CTT has small false positive rates on clean test data, minimal compute overheads when deployed, and can support complex security policies.

1 Introduction

Convolutional Neural Networks (CNNs) give the best performance on visual applications [1, 18, 32] and are now spreading into safety-critical fields, including autonomous vehicles [11], face recognition [34] and human action recognition [16]. However, small perturbations can be crafted to trigger misclassifications that are not perceptible by humans [14]. Researchers have demonstrated adversarial samples that can exploit face-recognition systems to break into smartphones [6] and misdirect autonomous vehicles by perturbing road signs [10]. These adversarial samples can be surprisingly portable. Samples generated from one classifier transfer to others, making them a potential large-scale threat to real-life systems.

Since most of these attacks use neural network gradient information to generate perturbations [14], the obvious defense is to improve the networks' classification robustness, such as training classifiers with these adversarial images. Such *adversarial training* significantly increases the performance of CNNs on adversarial samples but falls short in three ways. First, it assumes the defender has prior knowledge of the attacks; second, the defense is not certifiable; third, building a fully robust model is still an unsolved question [33]. In this paper, we look at a different defense strategy, namely adversarial sample detection. Researchers have shown that many adversarial samples are detectable, and detection methods normally hold no prior knowledge of attackers [26, 36]. We built on the existing Taboo Trap detection scheme [36], whose focus is on finding overly excited neurons being driven out-of-bound from a pre-defined range by adversarial perturbations. We propose a mechanism, the Certifiable Taboo Trap (CTT), that combines the original Taboo Trap detection with numerical bound propagation, making the detection bounds on CNN activation

---

*Equal Contribution

values certifiable against certain input perturbation sizes. For input perturbations at a particular l_∞ value, CTT can verify detection, meaning that CTT guarantees the detected samples are adversarial inputs.

In this paper, we propose three versions of CTT: lite, loose and strict. CTT-lite requires no additional fine-tuning on a pretrained model, and can provide basic protection against weak adversaries. CTT-loose retrains on a random set of selected activations with propagated numerical interval bounds, and provides a loose guarantee that all samples detected are adversarial. Finally, CTT-strict fine-tunes with more strict numerical interval bounds and thus is able to provide the same guarantee as CTT-loose on attackers with small l_∞ values; in addition, CTT-strict can verify detection on a pre-defined range of l_∞ values.

The contributions of this paper are:

- We introduce a novel certifiable detection scheme for adversarial samples.

- We show CTT-lite, a new detection method that is fine-tuning free but relatively limited in its defense capability. We demonstrate how to optimise detection boundaries through fine-tuning and introduce CTT-loose and CTT-strict. Assuming the test and training data distributions are the same, both detection schemes ensure that all detected samples are adversarial, CTT-strict even guarantees detections on adversarial samples with particular range of pre-defined l_∞ bounds.

- We show the detection results on all versions of CTT. For the first time, we empirically demonstrate how certifiable detection scheme (CTT-loose and CTT-strict) can have above 90% detection ratios on all attacks experimented on MNIST.

2 Related Work

The field of adversarial machine learning has seen a rapid co-evolution of attack and defense since researchers discovered adversarial samples [38]. The fast gradient sign method (FGSM) is an early adversarial attack that generates perturbations using the signs of the network gradients, and is still a simple yet effective way of finding adversarial samples [14]. The FGSM attack can be extended in an iterative way to look for smaller perturbations, giving the Projected Gradient Descent (PGD) Method or the Basic Iterative Method (BIM) [20, 25]. The Carlini & Wagner attack (CW) formulates an optimization problem, whose solution gives an adversarial sample [5]. However, a strong adversarial image is time-consuming to generate since it requires a large number of search iterations and binary search steps. Many of the attacks can change their optimization focus or be constrained on certain l_p norms in an iterative run. In our setup, we use the term l_p-bound attack to differentiate the same attack bounded by various l_p norms.

An interesting feature of adversarial samples is their transferability [38, 43, 14]. Adversarial samples that work well on a given neural network often transfer to a different type of network trained on the same dataset. This makes black-box adversarial attacks possible. Another way of finding black-box attacks is the gradient estimation method, which uses estimated gradient information instead of true gradients [2]. Estimation involves building an output distribution based on information queried from the target model.

Many defenses against adversarial attacks have been proposed, most of them relying on improving classification robustness. Adversarial training adds adversarial samples to the training set, so that the model becomes more robust at classification boundaries [14, 20]. Pang et al. use an ensemble of models to increase decision robustness [30], while Mustafa et al. use class-wise disentanglement to restrict feature maps crossing the decision boundaries [29]. However, Schott et al. showed that even building robust classification on the small MNIST data remains an unsolved question [33]. They also proposed the analysis and synthesis (ABS) method using class-conditioned data and demonstrate better robustness on the MNIST classification task.

Many researchers have tried to detect adversarial samples [26, 24, 27, 35]. Magnet claims that detection is possible by inspecting the reconstruction error of a trained autoencoder [26]. SafetyNet proposed SVM classifiers to recognize adversaries through neural activation patterns [24]. However, both of these detection methods rely on auxiliary components, which have two main problems. First, they impose a significant computational overhead. Second, an adversary might obtain a copy of the defense and devise an adversarial sample to defeat it [4, 7].

Another efficient detection scheme is the Taboo Trap [36], where a random subset of neurons are constrained in training and an alarm is set off when some threshold of them become overly excited. This imposes no extra runtime computational costs, and the constrained subset of neurons can be randomly picked, giving what amounts to a key that can be different each time the network is trained. This makes Black-box attacks more challenging as there can be multiple independently-keyed networks each of which is vulnerable to different adversarial samples [37]. Our work builds on the Taboo Trap, and answers the question of how to make adversarial sample detections certifiable. It also

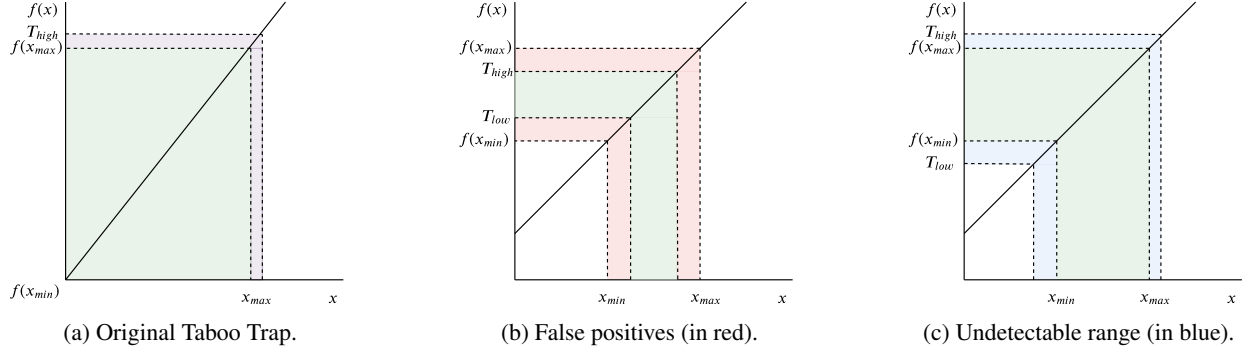(a) Original Taboo Trap.   (b) False positives (in red).   (c) Undetectable range (in blue).

Figure 1: Taboo Trap visualisation. If x is from the original data distribution, a strict bound causes them to be detected as adversarial samples, the red area shows the false positive samples (middle figure). If x is an adversarial sample, loose bounds cause detection fail on adversarial samples with small l_∞ values (blue part in figure on the right).

estalishes the optimal numerical range limit on neurons, and thus significantly improves the detection performance of the Taboo Trap.

Our work can also be viewed as being related to certifiable robustness where the prediction of a data point x is verifiably constant with perturbations of a certain l_p norm. When queried with the input data x, x will be perturbed by isotropic Gaussian noise and multiple inference runs are executed on a base classifier f [8, 23], in this way, the returned classification provides the most probable prediction made by f with a Gaussian corrupted x. Meanwhile, certification of adversarial samples can be achieved using bound interval propagation, which is becoming established as a means of formal verification of neural networks [15, 9, 39, 40, 13, 28, 17]. Several prior works have studied efficient relaxation methods for computing tight bounds on the neural network outputs [39, 40]. Our Certifiable Taboo Trap uses bound-interval propagation, but its focus is on certifying out-of-bound values in a set of randomly sampled intermediate activations. The interval bounding is a simple integral bound so the computation overhead is minimised [28].

3 Method

3.1 Taboo Trap: A Practical View

The method shown here extends the Taboo Trap originally presented by [36, 37]. First, we will explain the Taboo Trap method and then demonstrate the extension made for producing a relaxed guarantee that a certain l_∞ bound attacker will always be detected.

The Taboo Trap is based on the idea that neural network activations can be forced to form a distribution when trained with extra regularisations. Regularisations are based on activation values, and bound a set of activations inside a certain numerical range. No training set inputs trigger this chosen set of activation values to be out of range. So if one of these 'taboo' activations is observed, it signals that the current input may be adversarial. As different instances of the model can be trained with different taboo sets, the authors coined a term of a *transfer function*, which essentially served as a neural network key. In the original Taboo Trap, Shumailov et al. made use of the nth-max percentile activation bounds profiled from a trained network [36]. They later used polynomial keys [37]. Yet, the detection rates reported were less than ideal: the nth-max percentile function only detects weak attackers, while polynomial-based detectors show good detection rates on transfer attacks but perform worse under direct attack.

The Taboo Trap authors hypothesised that its performance is related to the choice of transfer functions, yet could not explain why some attackers could not be detected. While their experiments show a practical ability to detect adversaries, there is little theoretical understanding of how and why it worked.

3.2 Taboo Trap: A Theoretical View

In this section, we provide a theoretical understanding of how operating on the high dimensional activation space can detect adversarial samples. Assume that we have a linear function $f(x) = ax + b$ for illustration simplicity. The simple integral bound of the linear function with input bounded between $x_{\min}$ and $x_{\max}$ is bounded by $f(x_{\min})$ and $f(x_{\max})$.

Figure 1a presents how the original Taboo Trap will instrument function f with a nth max percentile transfer function. $x_{\min}$ and $x_{\max}$ represent the minimum and maximum values x can take. Since network inputs are bounded, the

intermediate layers should receive inputs that are also bounded, regardless of non-linearities. Being monotonic functions, $f(x_{\min})$ and $f(x_{\max})$ present the minimum and maximum values that the function f can naturally assume. If T_{high} represents the Taboo Trap threshold; we have:

$$\begin{cases} f(x) \leq T_{\text{high}} & \text{Benign} \\ f(x) > T_{\text{high}} & \text{Malicious} \end{cases} \tag{1}$$

We define an adversarial sample $\hat{x} = x + \epsilon$, with its l_∞ norm having the size of ϵ. With different detection thresholds (T_{high}), we can have natural samples becoming false positives or adversarial samples becoming undetectable. Figure 1b shows the scenario when $T_{\text{high}} < f(x_{\max})$: there exists a clean sample x with an output $f(x)$ being in between T_{high} and $f(x_{\max})$. This triggers natural samples to be misclassified as adversarial (false positives). Figure 1c presents the case that $T_{\text{high}} > f(x_{\max})$: adversarial samples $\hat{x}$ can generate output $f(\hat{x})$ smaller than T_{high} so that it becomes undetectable by the Taboo Trap framework. In summary:

$$\begin{cases} T_{\text{high}} > f(x_{\max}) & \text{Missed detection} \\ T_{\text{high}} < f(x_{\max}) & \text{False positives} \end{cases} \tag{2}$$

Consider $r = |f(x_{\max}) - T_{\text{high}}|$, it means

- if r equals to zero, the adversarial samples will always get detected.
- for a given r it is easy to compute what type and how many of perturbations will go undetectable.
- as mentioned by Shumailov et al. , there is a direct measurable trade-off between false positives, accuracy and detection rate.

Using the method defined above, it becomes apparent that all monotonic transfer functions should theoretically work in Taboo Trap, and have a trade-off between accuracy, false positive and detection rates.

Perturbations can also exist in the range between $x_{\min}$ and $x_{\max}$. The original Taboo Trap paper observed that better detector performance is achieved by setting a small threshold value, yet training becomes hard. Our hypothesis is that reducing the distance between $x_{\min}$ and $x_{\max}$ leads to a reduced number of perturbations in the natural image range.

It is also worth noting that detection occurs on post-ReLU activation values, and only the positive numerical range and the positive numerical threshold (T_{high}) are considered. For simplicity, we use T_l to represent a layer-wise threshold scalar in later descriptions.

3.3 Interval Bound Propagation

For simplicity, we consider a feed-forward CNN F consisting of a sequence of convolution layers, where the lth layer computes output feature maps $\mathbf{x}_l \in \mathbb{R}^{C_l \times H_l \times W_l}$. $\mathbf{x}_l$ is a collection of feature maps with C_l channels of $H_l \times W_l$ images.

The first stage of CTT is to compute the activation bounds from a pretrained network. Given the pretrained weights and the numerical bounds of inputs, CTT computes the numerical bounds for each layer in the CNN. Assuming the a set of lower and upper bound for layer l is $(B_l^{\text{low}}, B_l^{\text{up}})$, where B_l^{low} is the lower bound and B_l^{up} is the upper bound respectively, we have

$$\begin{aligned} B_{l+1}^{\text{low}} &= \text{Conv}_{\text{b}}(W_l, B_l^{\text{low}}) \\ B_{l+1}^{\text{up}} &= \text{Conv}_{\text{b}}(W_l, B_l^{\text{up}}) \end{aligned} \tag{3}$$

Notice B_0^{low} and B_0^{high} will be the boundaries on the input, obtained from profiling on the natural input data samples. Both B_l^{low} and B_l^{up} have the same dimensions as $\mathbf{x}_l$. The interval bound propagation in Equation (3) can be seen as a series of abstract interpolations in a convolution (Conv_{b}) [40, 28]. Given scalar bounds $m_l \leq m \leq m_h$ and $n_l \leq n \leq n_h$, we define an operation $(m_l, m_h) \cap (n_l, n_h)$ produces a tighter bound $p_l = \max(m_l, n_l)$ and $p_h = \min(m_h, n_h)$:

$$(m_l, m_h) \cap (n_l, n_h) = (\max(m_l, m_l), \min(n_h, n_h)) \tag{4}$$

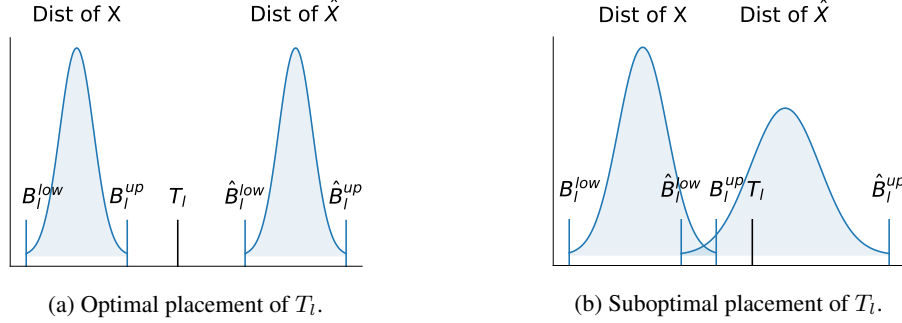(a) Optimal placement of T_l.   (b) Suboptimal placement of T_l.

Figure 2: Placements of the detection threshold T_l with different boundaries from both the natural activations (X) and the adversarial activations ($\hat{X}$). This indicates that both the numerical value of T_l and the two distributions should be optimised using fine-tuning.

This is equivalent to abstract interpolation in the interval domain (the box domain) [28]. Notice the bound propagation can also be performed for adversarial inputs, where the upper bound of the input becomes $\hat{B}_0^{\mathrm{up}} = B_0^{\mathrm{up}} + \epsilon$ and ϵ is the size of the l_∞ norm. We then define $(\hat{B}_l^{\mathrm{low}}, \hat{B}_l^{\mathrm{up}})$ to be a pair of upper bound and lower bound for layer l for adversarial inputs with an l_∞ budget of ϵ.

Considering the case in the middle layer l, we obtain a particular activation value x and its values across all input data distributions can be seen as a set X. Meanwhile, its values for all adversarial samples with an adversarial perturbation can be viewed as a set $\hat{X}$. For convenience, we call X the natural set and $\hat{X}$ the adversarial set. Figure 2 shows the placements of the detection threshold T_l. In the ideal case, if the distributions of the natural set (X) and the adversarial set ($\hat{X}$) are disjoint, the optimal placement of T_l is that $B_l^{\mathrm{up}} <= T_l <= \hat{B}_l^{\mathrm{low}}$. However, in practice, the natural set and the adversarial set might overlap (Figure 2b), meaning that there is only a sub-optimal placement option $B_l^{\mathrm{up}} \leq T_l \leq \hat{B}_l^{\mathrm{up}}$. For these two threshold placements, we conclude:

- Optimal placement of T_l ($B_l^{\mathrm{up}} \leq T_l \leq \hat{B}_l^{\mathrm{low}}$) ensures that all adversarial samples with l_∞ norm at the size of ϵ are detectable (Figure 2a).

- Both optimal and suboptimal placements ($B_l^{\mathrm{up}} \leq T_l \leq \hat{B}_l^{\mathrm{up}}$) of T_l ensure that all detected samples are adversarial regardless of the perturbation size (Figure 2b).

The above claims are true if and only if the following assumption holds: *The test data distribution falls inside the training data distribution.* In other words, the test data falls in the range of the maximum and minimum bounds profiled from the training dataset. The rest of this section discusses methodologies we used to ensure that placements of T_l are near-optimal. In Section 3.4, we show a training-free method of finding the position of T_l. In Section 3.5, several losses are discussed that help to force the placement of T_l towards optimal and suboptimal.

3.4 Taboo Trap for Free

One major bottleneck of defending adversarial samples is the training overhead. Classic methods like adversarial training increase model robustness by training with additional adversarial data points and thus significantly increase the training time. CTT can be deployed without any additional fine-tuning, and we name this detection mode CTT-lite.

We previously introduced the concept of a detection threshold value. Recall the definition of a particular layer's output activations $\mathbf{x}_l$, CTT uses a randomised binary mask $\mathbf{m}_l^d$ that is the same size of $\mathbf{x}_l$ to decided on which activation values to restrict on. Unlike [37] who used different transfer functions as keys, in this work we represent different keys as different subsets of neurons that are instrumented with CTT. We find that such construction has all of the benefits described by [37] originally. Practically, CTT only detects on $\mathbf{x}_l \cdot \mathbf{m}_l^d$, where $\cdot$ is a Hadamard product (element-wise multiplication) between matrices.

CTT-lite simply places T_l at the upper boundary of the natural set so that $T_l = B_l^{\mathrm{up}}$. In the original Taboo Trap setup, as in Section 3.2, this effectively means $r = |f(x_{\max}) - T| = 0$. So the only additional computation is to perform the interval bound propagation for deducing the value of T_l in each layer, and no additional training is required. Note that as the bounds are computed for the training dataset it will have false positives for the evaluation dataset.

Algorithm 1 Certifiable Taboo Trap finetuning process
___

Inputs: $\alpha, \beta, \theta, f, x, y, \epsilon, E$
$\mathbf{m}^d = \text{RandomMaskGen}(\beta)$
for $e = 0$ **to** $E - 1$ **do**
    $L = \text{CrossEntropy}(y, f(x))$
    $B = \emptyset, \hat{B} = \emptyset$
    for $l \in \text{Layers}(f)$ **do**
        $(B_l^{\text{up}}, B_l^{\text{low}}) = \text{BoundPropagate}(l, x, f)$
        $(\hat{B}_l^{\text{up}}, \hat{B}_l^{\text{low}}) = \text{BoundPropagate}(l, x \pm \epsilon, f)$
        $B = B \cup (B_l^{\text{up}}, B_l^{\text{low}})$
        $\hat{B} = \hat{B} \cup (\hat{B}_l^{\text{up}}, \hat{B}_l^{\text{low}})$
    end for
    $L_D, L_V = \text{ComputeRegLoss}(B, \hat{B}, f(x), \mathbf{m}^d)$
    $\alpha = \text{Anneal}(\alpha, e)$
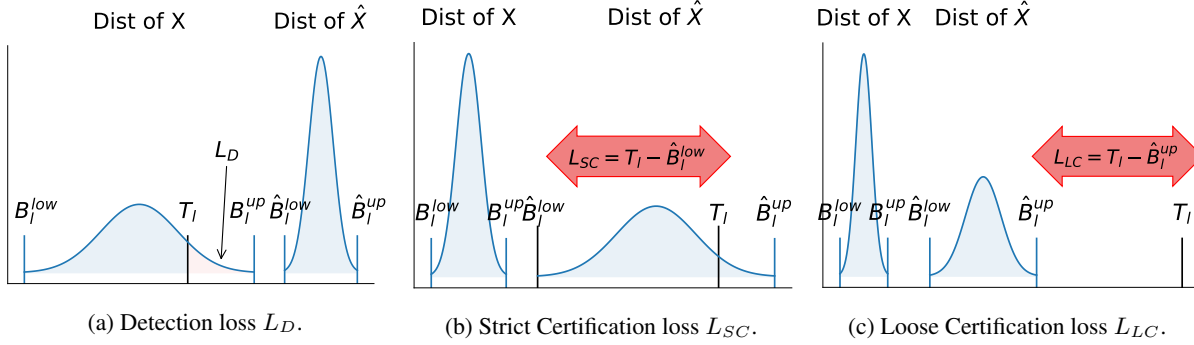 $\text{Opt}_\theta(L + \alpha(L_D + L_V))$
end for

(a) Detection loss L_D.   (b) Strict Certification loss L_{SC}.   (c) Loose Certification loss L_{LC}.

Figure 3: An illustration of CTT regularisation losses. The detection loss (L_D) ensures no natural samples are detected. Strict certification loss encourages the placement of T_l to be optimal, while loose certification loss helps T_l to achieve the suboptimal placement.

3.5 Fine-tuning with CTT Losses

Fine-tuning networks further with CTT losses can introduce a better separation between the natural and the adversarial sets. Unlike adversarial training, CTT fine-tuning operates on the original data; we do not generate any adversarial inputs to train with the model, so the training overheads are lower for CTT. We present three losses related to interval bounds that are considered as regularisations in our CTT detection. The three losses are presented in Figure 3, and they are: 1) Detection loss L_D, 2) Strict certification loss L_{SC}, 3) Loose certification loss L_{LC}.

Consider a masking function $\mathbf{m}_l = M(\mathbf{x}_l, T_l)$, the output $\mathbf{m}$ is a binary mask of which its elementwise entry is 1 if its corresponding elementwise entry in $\mathbf{x}$ is bigger than a scalar T_l, and otherwise is 0. The detection loss L_D is a sum of all activation values picked by the taboo selection mask $\mathbf{m}_l^d$ that are greater than the detection threshold T_l. The verification losses are simply the distance between the detection threshold and the bound when the threshold is bigger than the bound. Considering a network with N layers, we have:

$$L_D = \sum_{l=0}^{N-1} \text{sum}(\mathbf{x}_l \cdot \mathbf{m}_l^d \cdot M(\mathbf{x}_l, T_l)) \tag{5}$$

$$L_{SC} = \sum_{l=0}^{N-1} \text{sum}(\mathbf{m}_l^d \cdot M(\hat{B}_l^{\text{low}}, T_l) \cdot (T_l - \hat{B}_l^{\text{low}})) \tag{6}$$

$$L_{LC} = \sum_{l=0}^{N-1} \text{sum}(\mathbf{m}_l^d \cdot M(\hat{B}_l^{\text{up}}, T_l) \cdot (T_l - \hat{B}_l^{\text{up}})) \tag{7}$$

The function sum produces the sum of all entries of a high dimensional tensor that is the result of convolutions (activations). Recall we previously defined the optimal and suboptimal placements of T_l in Section 3.3, the minimization of different combination of CTT regularisation losses provide:

- If $L_D = 0$ and $L_{SC} = 0$, we are achieving the optimal placement of T_l. All adversarial inputs with its l_∞ norm equals to ϵ are detectable, and all detected samples are adversarial samples regardless of the perturbation size. Given that test data falls into the train data distribution.
- If $L_D = 0$ and $L_{LC} = 0$, we are achieving the suboptimal placement of T_l, all detected samples are adversarial samples regardless of the perturbation size. Given that test data falls into the train data distribution.

Table 1: A comparison between CTT-lite, CTT-loose, CTT-strict, AdvTrain [20], Ensemble [30] and PCL [29] on the MNIST dataset. Acc means accuracy and Det means detection rate on adversarial samples.

Attack	Param	Baseline Acc	AdvTrain Acc	Ensemble Acc	PCL Acc	CTT-lite Acc	Det	l_2	CTT-loose Acc	Det	l_2	CTT-strict Acc	Det	l_2
No Attack		99.1	99.5	99.5	99.3	99.1	1.9	-	98.5	1.6	-	98.9	1.1	-
FGSM	$\epsilon = 0.1$	70.9	73.0	96.3	96.5	70.9	1.4	2.08	25.0	100.0	1.98	61.1	100.0	1.99
	$\epsilon = 0.2$	21.9	52.7	52.8	77.9	21.9	1.0	4.14	15.0	100.0	3.89	32.7	100.0	3.90
BIM	$\epsilon = 0.1$	44.2	62.0	88.5	92.1	44.2	1.0	1.13	0.0	100.0	0.38	0.15	100.0	0.75
	$\epsilon = 0.15$	4.2	18.7	73.6	77.3	4.2	0.8	1.48	0.0	100.0	0.50	2.0	100.0	0.97
PGD	$\epsilon = 0.1$	51.0	62.7	82.8	93.9	51.0	1.2	1.50	1.0	100.0	1.24	13.4	100.0	1.35
	$\epsilon = 0.2$	0.0	31.9	41.0	80.2	0.0	1.1	2.73	0.0	100.0	2.43	0.9	100.0	2.53
C&W	$c = 0.1$	99.6	71.1	97.3	97.6	99.6	25.0	0.05	34.0	90.5	0.06	79.6	91.2	0.05
	$c = 1.0$	99.6	39.2	78.1	91.2	99.6	1.1	0.05	34.3	93.3	0.07	79.7	96.1	0.06

We present the detailed fine-tuning algorithm in Algorithm 1. The finetuning function takes a hyperparameter α, this controls how strong the regularisation is in the optimization procedure (Opt). In practice, it is necessary to anneal (Anneal) the value of α with respect to the number of epoch e. The other hyperparameter β is a probability between 0 to 1 that is later used to produce a set of masks $\mathbf{m}^d$ for each layer's activations. In the meantime, the fine-tune function considers a neural network f with trained parameters θ; x and y are the training data samples and their labels respectively. In addition, we need a pre-defined perturbation size ϵ for adversarial bound construction and E represents the maximum number of epochs we would like to fine-tune for. Function CrossEntropy essentially computes the classification loss L based on the input training data.

Consider a neural network f parameterised by θ. For each layer in the neural network f, we perform the bound propagation (BoundPropagate) as described in Section 3.3. The bounds for both the adversarial set of inputs and the natural set of inputs of each layer are accumulated for computing the regularisation loss using the function ComputeRegLoss. Note that the adversarial set represents the set of inputs with a particular l_∞ norm, so there is no actual generation of adversarial samples. The function ComputeRegLoss produces two losses L_D and L_C; the value of L_C can be calculated to be equal to whether L_{SC} or L_{LC} (Equation (6) and Equation (7)) depending on whether we use CTT-strict or CTT-loose. Since Algorithm 1 is only a high level overview, we did not distinguish between L_{SC} and L_{LC}, but call them in general L_C in Algorithm 1. It is worth to note that L_{SC} is a stronger regularisation than L_{LC}, so adding both regularisations is theoretically equivalent to adding only L_{SC}. The pre-defined parameter ϵ determines a trade-off between accuracy, detection ratios and adversarial accuracy. In practice, we determine the value of ϵ using a grid search spanning values from 10^{-5} to 10^{-1}, and determine its value based on the optimal performance in accuracy and detection ratio under a simple FGSM attack with fixed l_0. We explain this trade-off in details in our supplementary material.

4 Evaluation

4.1 Networks, Datasets and Attacks

We evaluate the proposed Certifiable Taboo Trap (CTT) on two different image datasets, MNIST [21] and CIFAR10 [19]. The MNIST dataset consists of images of hand-written digits and the number of output classes is 10. The CIFAR10 dataset is a task of classifying 60000 images into 10 classes. We use the LeNet5 [22] architecture for MNIST, and evaluate an efficient CNN architecture (MCifarNet) from Mayo [42] that achieved a high classification accuracy using only 1.3M parameters.

We consider gradient-based FGSM [14], FGM [14], BIM [20], PGD [20] and C&W [5] attacks with various attack parameters. These attacks can be seen as a collection of l_∞ and l_2 based attacks. In addition, we provide results in

Table 2: A comparison between CTT-loose, CTT-strict, AdvTrain [20], Ensemble [30] and PCL [29] on the Cifar10 dataset. Acc means accuracy and Det means detection rate on adversarial samples.

Attack	Param	Baseline Acc	AdvTrain Acc	Ensemble Acc	PCL Acc	CTT-loose						CTT-strict		
						Acc	Det	l_2	Acc	Det	l_2	Acc	Det	l_2
No Attack		89.1	84.5	90.6	91.9	86.2	3.4	-	86.3	6.4	-	86.1	3.0	-
FGSM	$\epsilon = 0.02$	33.6	44.3	61.7	78.5	18.6	95.7	1.07	16.8	98.5	1.08	16.1	96.4	1.06
	$\epsilon = 0.04$	22.4	31.0	46.2	69.9	7.6	93.6	2.00	7.2	94.2	2.01	6.0	93.1	2.06
BIM	$\epsilon = 0.01$	13.5	22.6	46.6	74.5	0.5	9.0	0.15	0.0	14.1	0.16	1.1	10.9	0.16
	$\epsilon = 0.02$	1.5	7.8	31.0	57.3	0.0	14.2	0.21	0.0	25.9	0.20	0.0	17.2	0.21
PGD	$\epsilon = 0.01$	24.0	24.3	48.4	75.7	0.1	10.4	0.34	2.9	24.3	0.34	2.0	16.6	0.34
	$\epsilon = 0.02$	2.9	7.8	30.4	48.5	0.0	40.8	0.65	0.0	70.3	0.65	0.0	49.9	0.65
C&W	$c = 0.01$	13.5	40.9	54.9	65.7	0.2	12.9	0.09	0.1	23.4	0.10	0.5	14.5	0.09
	$c = 0.1$	13.3	25.4	25.6	60.5	0.3	13.3	0.09	0.1	25.9	0.10	0.5	13.7	0.09

Table 3: A comparison between CTT-lite, CTT-loose, CTT-strict, Madry et al. [25], Sitatapatra [37], ABS and Binary ABS [33] on the MNIST dataset. For detection based defense, we show results in the form of $a(d)$, where a is accuracy and d is detection rate. GE represents gradient estimation.

	CNN	Madry et al.	Binary ABS	ABS	Sitatapatra	CTT-loose	CTT-strict
No Attack	99.1%	98.8%	99.0%	99.0%	99.2% (2%)	99.1% (0.5%)	98.8% (1.3%)
l_2-metric ($\epsilon = 1.5$)							
FGM	48%	96%	-	-	2% (3%)	4% (99%)	21%(100%)
FGM w/ GE	42%	88%	68%	89%	4% (7%)	0% (100%)	25%(100%)
Deepfool	18%	91%	-	-	12% (1%)	0% (100%)	77% (95.6%)
Deepfool w/ GE	30%	90%	41%	83%	6% (2%)	0% (100%)	76.5% (94.4%)
L2 BIM	13%	88%	-	-	0% (0%)	0% (100%)	0% (100%)
L2 BIM w/ GE	37%	88%	63%	87%	0% (3%)	0% (100%)	0% (100%)
l_∞-metric ($\epsilon = 0.3$)							
FGSM	4%	93%	-	-	2%(3%)	1% (99%)	2%(100%)
FGSM w/ GE	21%	89%	85%	34%	0%(2%)	0% (100%)	4% (100%)
BIM	0%	90%	-	-	0%(1%)	0% (100%)	0% (100%)
BIM w/ GE	37%	89%	86%	13%	0%(1%)	0% (100%)	0% (100%)

both White-box and Black-box settings. For Black-box attacks, we use gradient estimation with the coordinate-wise finite-difference method, similar to Schott et al. [33]. The attack implementations are from Fooblox [31].

4.2 Attackers with Various Capabilities and Various Norm Bounds

Attacks can be evaluated very differently, and we offer two sets of evaluations for a thorough comparison with existing defense methods. In the first set, we run attacks with fixed parameters and a fixed number of iterations. In the second se, we enable early stopping for iterative attacks so that perturbation sizes are fixed. In addition, we also provide a set of evaluation with Black-box attacks using gradient estimation. We used $\epsilon = 3 \times 10^{-3}$ for MNIST networks, and $\epsilon = 10^{-4}$ for CIFAR10 networks. These values were determined from a grid search; there is a detailed discussion of the grid search and an evaluation of using different ϵ in the supplementary material. In addition, we show the detailed hyperparameter configurations of α, β, E and ϵ (Algorithm 1) in the supplementary material.

In Table 1 and Table 2, we present comparisons between CTT and various robust adversarial training schemes, including AdvTrain [20], Ensemble [30] and PCL [29]. In this setup, we run attacks with fixed parameters and measure the accuracy, detection ratios and l_2 norms of the adversarial samples. BIM and PGD iterated for 10 times with a step size of $\epsilon/10$; CW has an iteration step of 1000, an learning rate of 0.01, a confidence value of 0.1 and a binary search step of 1. Notice we present the baseline accuracy for the networks on which we evaluate. The baseline accuracy will be the same as CTT-lite, since it involves no re-training of the model. CTT-lite provides limited protections against adversarial attacks. CTT-loose and CTT-strict, however, show above 90% detection ratios across all examined attacks in Table 1. In addition, both detection schemes provide a degree of certifiability on the detected adversarial samples. The detection ratios when no attacks are applied are the false positives. There exists a trade-off between the false positive rates and the detection ratios. As presented in Table 2, the two versions of CTT-loose have different false positive rates, and offer different detection capabilities. We presents a full analysis of this trade-off in the supplementary material. Table 2 shows our detection scheme outperform robust networks on FGSM, however, provides relatively worse performance when l_2 norms are low. First, our detection offers certifiability which is not seen in any of the work compared. Second,

the work compared does not report the l_2 norm, attacks with different random starts may cause a difference in l_2 norms and also the attacking quality.

To further evaluate the CTT system, we conduct a comparison to Madry et al., Sitatapatra [37] ABS and Binary ABS [33] under both White- and Black-Box attacks on the MNIST dataset. This time, we provide a noise budget to each attack. The Black-Box attacks are constructed using gradient estimation, we see almost all CTT-loose and CTT-strict results show above 90% detection ratios on adversarial samples while keeping the false positives low. Our detection results outperform all other competitors focusing solely on improving model robustness. An important observation is that our detection method reduces the adversarial accuracy of the neural network model. This phenomenon is apparent in Table 1, as all robustness-based defenses have higher accuracy in comparison to CTT on adversarial images. Intuitively, CTT enforces the natural and the adversarial sets to be separated by the detection thresholds. The CTT models are thus more sensitive to adversarial samples because of this enforcement — we observe that selected neurons get suppressed for natural and get non-zero values for adversarial inputs. Furthermore, our detection is certifiable based on an assumption that the test and train data follows the same distribution. In theory, if this assumption is true, CTT-strict will show 100% detection on all attacks that are above a certain given l_∞; which is exactly the case shown in Table 1 with l_∞-based attacks. For l_2-based attacks, it is hard to ensure every pixel is under the given certifiable limit, however, our method practically capture many adversaries with high detection rates.

4.3 Runtime Overheads and Security Protocols

The proposed CTT system has low running overheads in comparison to other detection systems (SafetyNet [24] and MagNet [26]), we present the run-time comparison in appendix. It is similar to Sitatapatra [37], which is another derivative of Taboo Trap; CTT supports the concept of embedding keys in each neural network to diversify models under adversarial attack. The key is embedded via the mask and can support complex security protocols; a detailed analysis of key attribution and runtime overheads can be found in Shumailov et al. and these advantages are equally applicable to CTT.

5 Conclusion

In this paper, we presented the Certifiable Taboo Trap CTT), a new way to defend neural networks against adversarial samples by detecting them. We discussed three different modes which provide different detection capabilities and levels of certifiability at different training costs. All variants of CTT have a small run-time overhead, and can be customised with the equivalent of cryptographic keys. The stronger variants of CTT have extra training but this is used to characterise propagation bounds rather than to defend against specific adversarial samples, yielding a more flexible and general defense mechanism.

Appendices

A   Training procedure

In this section we explain how to train a CTT instrumented model. First, most of the commonly used optimisers are suitable for CTT training. However, it should be noted that there exists an interaction between the CTT penalty (the additional loss term introduced by CTT) and the weight decay of the optimizer. Although we have not evaluated this interaction formally, we find it easier to train models when the weight decay is either turned off or set to a very small value. The optimizer used in our experiments is RMSProp.

The annealing procedure for CTT parameters is important for convergence. The parameter α determines the strength of the CTT penalty, and we increase α iteratively by a factor of β every t training epochs. For both MNIST and FashionMNIST, we used $t = 6, \beta = 0.005$. For CIFAR10, we used $t = 30, \beta = 0.001$. We find that the best way to train the models is to first optimise L_V, i.e. make sure that neurons have a bound larger than T_l and then start iteratively increasing α. We hypothesise that this works in line with recent findings that there exist a number of connected convergence clusters with similar performance [12] with a path between them. Iteratively increasing α allows us to keep convergence, while maintaining low L_V loss and decreasing the false positive rate.

B   Parameter Selection

In this section we try to explain intuition behind CTT and the instrumentation parameter (ϵ) choice. Algorithm 1 in the paper presents the whole procedure we have used to successfully train both CTT-loose and CTT-strict.

First, the parameter ϵ can be thought of as a *detectability* certification of an adversarial sample. It defines the minimum theoretical perturbation size for which the detector should work. In other words, when training the classifier with CTT, we generate adversarial bounds up to a limit of ϵ. Rather than generating adversarial samples, we use a natural sample perturbed by ϵ. The CTT loss tries to ensure that when adversarial samples $X \pm \epsilon$ are considered, the detector neurons can be turned on.

CTT may be understood in contrast with the work of Cohen et al. in certifiable robustness [8]. Certifiable robustness aims at making natural sample behaviour stay in a pre-formed l_p ball, so that model behaviour is stable in a natural range of values. CTT, on the other hand, aims at detecting illegal behaviours outside of this l_p ball, so that behaviour outside of the natural range is unstable. The intuition is that the smaller you make this l_p norm for CTT, the the easier we can detect adversarial behaviours.

Figure 4 shows the trade-off between detector performance and ϵ-choice using CTT-loose. First, the pre-defined ϵ does not guarantee that all adversarial samples above this ϵ will be detected (only CTT-strict guarantees this). Second, there is an optimal ϵ we can choose to maximize the detectability. Third, unlike adversarial training, CTT does not rely on a particular attack during training. As shown in Figure 4, the performance of different attacks (PGD and FGSM) shows almost no difference and the attack quality seems to be only related to the perturbation size rather than generation procedure. Finally, the left-most point shown in Figure 4 refers to $\epsilon = 10^{-5}$. It seems that for a given architecture and a given dataset there exists a smallest ϵ one could successfully train the model for. For MNIST with LeNet5 we struggled to find a reproducible way to train the model for epsilons below 0.0007.

C   FashionMNIST vs MNIST

MNIST is a popular benchmark, but is known to be relatively simple [21]. Xiao et al. proposed FashionMNIST [41], a more complex, yet still simple toy dataset. In this section we report on results of CTT-loose instrumentation of LeNet5 networks solving FashionMNIST with $\epsilon = 0.001$, meaning that the adversarial set includes perturbed images with an l_∞ size of 0.001.

In addition to the attacks presented in the evaluation section, we also show here the results for a decision-based attack [3]. The attack itself is particularly interesting as it is not based on any gradient information, meaning CTT detection is not network-information specific. For this attack, we use 25 trials per iteration and vary the number of iterations.

Table 4 shows the results of attacking CTT-loose instrumented LeNet5. In the evaluation section of the paper we have shown that for MNIST CTT detection was capable of capturing almost all of the adversarial samples. Unlike MNIST, CTT fails to detect all of the adversarial samples on FashionMNIST.
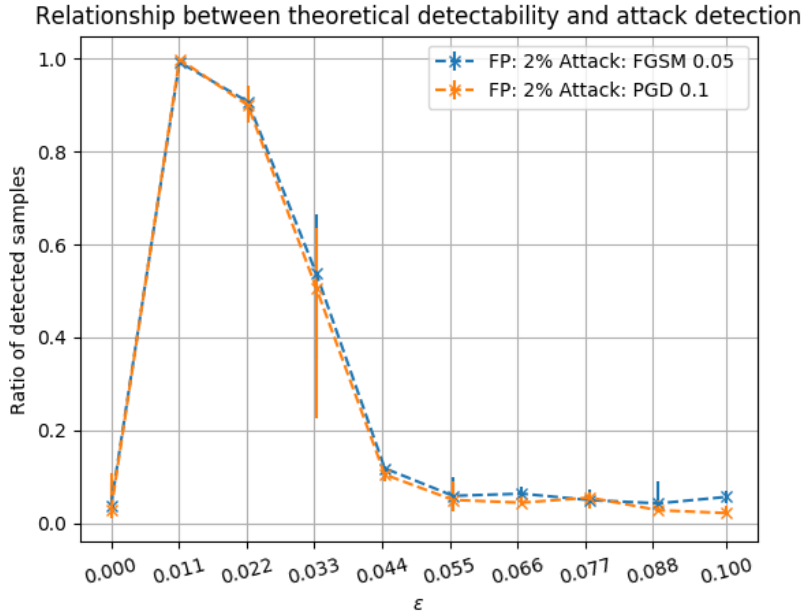
Figure 4: Trade-off between choices of ϵ and detector performance. There are five LeNet5 networks classifying MNIST, instrumented with CTT-loose with $T_l = 10^{-4}$ with a given ϵ. The networks are trained to a false positive rate of 2%. Points show median performance, whereas error bars refer to standard deviations of the 5 networks.

As already noted, there is a relationship between the attack perturbation size, dataset specifics, and the detectability of CTT. In the case of FashionMNIST, for the particular ϵ value, we find it shows relatively better detection rate for small l_2 values.

Table 4: CTT-loose instrumented LeNet5 network classifying FashionMNIST.

	θ	l_2	CTT-loose	
No Attack			85.3% (5.3%)	84.4% (2.7%)
FGSM	$\epsilon = 0.006$	0.10	64.73% (75.33%)	65.14% (39.66%)
	$\epsilon = 0.007$	0.12	60.79% (71.01%)	62.74% (39.68%)
	$\epsilon = 0.01$	0.17	52.32% (61.80%)	56.97% (38.55%)
	$\epsilon = 0.03$	0.52	22.62% (54.42%)	24.40% (44.52%)
	$\epsilon = 0.05$	0.88	11.72% (56.11%)	12.62% (49.79%)
	$\epsilon = 0.07$	1.23	6.61% (59.63%)	8.29% (51.51%)
Boundary	$i = 10$	1.96	0.00% (28.19%)	0.00% (20.19%)
	$i = 50$	1.62	0.00% (27.61%)	0.00% (23.44%)
	$i = 100$	1.23	0.00% (29.23%)	0.00% (24.52%)
	$i = 500$	0.24	0.00% (60.90%)	0.00% (38.94%)
	$i = 1000$	0.15	0.00% (65.31%)	0.00% (44.27%)

D   Detectability trade-off

In this section we show the impact of different false positive rates on the CTT-loose instrumentation. We use 5 LeNet5 networks and train each of them with the same CTT-loose restrictions but stop at different training times so that networks achieve different false-positive rates. Figure 5 presents the false positive rate trade-off two specific attacks, with false positive rates on the x-axis and detectability on the y-axis.

The relationship between detector performance and false positive rates indicates a trade-off of interest when applying CTT-loose in practice. With a slight increase of false positive rates (1% to 3%), we increase the detector performance by around 20%. Intuitively, this suggests first, that there exist inefficiencies in the internal representations of the neural network, where the network struggles to separate natural and non-natural samples. Second, this trade-off between false positive rates and detectability can occur because of imperfections of the training dataset. The natural training dataset

Figure 5: Trade-off between choices of false positive rates and detector performance. There are five LeNet5 networks classifying FashionMNIST, instrumented with CTT-loose with $T_l = 10^{-4}$ with a given $\epsilon = 0.005$. Points show median performance, whereas error bars refer to standard deviations.

involves imperfect, confusing images for the network, and thus causing a vague boundary between the natural and adversarial input sets. It should be noted that although this relationship exists across different datasets and models, its scaling seems to be dataset-dependent.

E Run-time overheads

Previously, Shumailov et al. demonstrated that Taboo Trap adds no extra inference cost and utilises zero additional device memory when deployed. In comparison, MagNet [26] and SafetyNet [24] show 20% and 3600% increases in terms of additional parameters when deployed [36]. As mentioned in our paper, CTT shares the same detection mindset as Taboo Trap, and thus enjoy the benefit of having zero extra cost in network inference as well. Unlike [36] however we instrument less than 0.1% of all neurons available in the network. That in turn means that fewer detector neurons are required for much better detection.

References

[1] Badrinarayanan, V., Kendall, A., and Cipolla, R. Segnet: A deep convolutional encoder-decoder architecture for image segmentation. *arXiv preprint arXiv:1511.00561*, 2015.

[2] Bhagoji, A. N., He, W., Li, B., and Song, D. Black-box attacks on deep neural networks via gradient estimation. *International Conference on Learning Representations Workshop (ICLR)*, 2018.

[3] Brendel, W., Rauber, J., and Bethge, M. Decision-based adversarial attacks: Reliable attacks against black-box machine learning models. In *International Conference on Learning Representations*, 2018. URL `https://openreview.net/forum?id=SyZI0GWCZ`.

[4] Carlini, N. and Wagner, D. Magnet and" efficient defenses against adversarial attacks" are not robust to adversarial examples. *arXiv preprint arXiv:1711.08478*, 2017.

[5] Carlini, N. and Wagner, D. Towards Evaluating the Robustness of Neural Networks. In *2017 IEEE Symposium on Security and Privacy (SP)*, pp. 39–57. IEEE, 2017.

[6] Carlini, N., Mishra, P., Vaidya, T., Zhang, Y., Sherr, M., Shields, C., Wagner, D., and Zhou, W. Hidden Voice Commands. In *25th USENIX Security Symposium (USENIX Security 16)*. USENIX Association, 2016.

[7] Chen, S., Carlini, N., and Wagner, D. A. Stateful detection of black-box adversarial attacks. *CoRR*, abs/1907.05587, 2019. URL http://arxiv.org/abs/1907.05587.

[8] Cohen, J., Rosenfeld, E., and Kolter, Z. Certified adversarial robustness via randomized smoothing. In *Proceedings of the 36th International Conference on Machine Learning*, 2019.

[9] Dvijotham, K., Gowal, S., Stanforth, R., Arandjelovic, R., O'Donoghue, B., Uesato, J., and Kohli, P. Training verified learners with learned verifiers. *arXiv preprint arXiv:1805.10265*, 2018.

[10] Eykholt, K., Evtimov, I., Fernandes, E., Li, B., Rahmati, A., Xiao, C., Prakash, A., Kohno, T., and Song, D. Robust Physical-World Attacks on Deep Learning Visual Classification. In *Proceedings of the IEEE Conference on Computer Vision and Pattern Recognition*, pp. 1625–1634, 2018.

[11] Fang, C.-Y., Chen, S.-W., and Fuh, C.-S. Road-sign detection and tracking. *IEEE transactions on vehicular technology*, 52(5):1329–1341, 2003.

[12] Fort, S., Hu, H., and Lakshminarayanan, B. Deep ensembles: A loss landscape perspective. *arXiv preprint arXiv:1912.02757*, 2019.

[13] Gehr, T., Mirman, M., Drachsler-Cohen, D., Tsankov, P., Chaudhuri, S., and Vechev, M. Ai2: Safety and robustness certification of neural networks with abstract interpretation. In *2018 IEEE Symposium on Security and Privacy (SP)*, pp. 3–18. IEEE, 2018.

[14] Goodfellow, I. J., Shlens, J., and Szegedy, C. Explaining and harnessing adversarial examples. *International Conference on Learning Representations (ICLR)*, 2015.

[15] Gowal, S., Dvijotham, K., Stanforth, R., Bunel, R., Qin, C., Uesato, J., Mann, T., and Kohli, P. On the effectiveness of interval bound propagation for training verifiably robust models. *arXiv preprint arXiv:1810.12715*, 2018.

[16] Ji, S., Xu, W., Yang, M., and Yu, K. 3d convolutional neural networks for human action recognition. *IEEE transactions on pattern analysis and machine intelligence*, 35(1):221–231, 2013.

[17] Katz, G., Barrett, C., Dill, D. L., Julian, K., and Kochenderfer, M. J. Reluplex: An efficient smt solver for verifying deep neural networks. In *International Conference on Computer Aided Verification*, pp. 97–117. Springer, 2017.

[18] Krizhevsky, A., Sutskever, I., and Hinton, G. E. ImageNet classification with deep convolutional neural networks. In *Advances in neural information processing systems*, pp. 1097–1105, 2012.

[19] Krizhevsky, A., Nair, V., and Hinton, G. The CIFAR-10 dataset. 2014.

[20] Kurakin, A., Goodfellow, I., and Bengio, S. Adversarial machine learning at scale. 2017.

[21] LeCun, Y., Cortes, C., and Burges, C. MNIST handwritten digit database. 2, 2010.

[22] LeCun, Y. et al. LeNet-5, convolutional neural networks. pp. 20, 2015.

[23] Lécuyer, M., Atlidakis, V., Geambasu, R., Hsu, D., and Jana, S. Certified robustness to adversarial examples with differential privacy. In *IEEE S&P 2019*, 2018.

[24] Lu, J., Issaranon, T., and Forsyth, D. A. Safetynet: Detecting and rejecting adversarial examples robustly.

[25] Madry, A., Makelov, A., Schmidt, L., Tsipras, D., and Vladu, A. Towards deep learning models resistant to adversarial attacks. 2018.

[26] Meng, D. and Chen, H. Magnet: A two-pronged defense against adversarial examples. In *Proceedings of the 2017 ACM SIGSAC Conference on Computer and Communications Security*, CCS '17, pp. 135–147, New York, NY, USA, 2017. ACM.

[27] Metzen, J. H., Genewein, T., Fischer, V., and Bischoff, B. On detecting adversarial perturbations. In *Proceedings of 5th International Conference on Learning Representations (ICLR)*, 2017.

[28] Mirman, M., Gehr, T., and Vechev, M. Differentiable abstract interpretation for provably robust neural networks. In *International Conference on Machine Learning*, 2018.

[29] Mustafa, A., Khan, S., Hayat, M., Goecke, R., Shen, J., and Shao, L. Adversarial defense by restricting the hidden space of deep neural networks. In *The IEEE International Conference on Computer Vision (ICCV)*, October 2019.

[30] Pang, T., Xu, K., Du, C., Chen, N., and Zhu, J. Improving adversarial robustness via promoting ensemble diversity. In Chaudhuri, K. and Salakhutdinov, R. (eds.), *Proceedings of the 36th International Conference on Machine Learning*, volume 97 of *Proceedings of Machine Learning Research*, pp. 4970–4979, 2019.

[31] Rauber, J., Brendel, W., and Bethge, M. Foolbox: A python toolbox to benchmark the robustness of machine learning models. *arXiv preprint arXiv:1707.04131*, 2017.

[32] Ren, S., He, K., Girshick, R., and Sun, J. Faster R-CNN: Towards real-time object detection with region proposal networks. In *Advances in neural information processing systems*, pp. 91–99, 2015.

[33] Schott, L., Rauber, J., Bethge, M., and Brendel, W. Towards the first adversarially robust neural network model on mnist. *International Conference on Learning Representations Workshop (ICLR)*, 2019.

[34] Schroff, F., Kalenichenko, D., and Philbin, J. Facenet: A unified embedding for face recognition and clustering. In *Proceedings of the IEEE conference on computer vision and pattern recognition*, pp. 815–823, 2015.

[35] Shan, S., Willson, E., Wang, B., Li, B., Zheng, H., and Zhao, B. Y. Gotta catch 'em all: Using concealed trapdoors to detect adversarial attacks on neural networks. *CoRR*, abs/1904.08554, 2019. URL `http://arxiv.org/abs/1904.08554`.

[36] Shumailov, I., Zhao, Y., Mullins, R., and Anderson, R. The taboo trap: Behavioural detection of adversarial samples. *arXiv preprint arXiv:1811.07375*, 2018.

[37] Shumailov, I., Gao, X., Zhao, Y., Mullins, R., Anderson, R., and Xu, C.-Z. Sitatapatra: Blocking the transfer of adversarial samples. 2019.

[38] Szegedy, C., Zaremba, W., Sutskever, I., Bruna, J., Erhan, D., Goodfellow, I. J., and Fergus, R. Intriguing properties of neural networks. *CoRR*, abs/1312.6199, 2013.

[39] Wang, S., Pei, K., Whitehouse, J., Yang, J., and Jana, S. Efficient formal safety analysis of neural networks. In *Advances in Neural Information Processing Systems*, pp. 6367–6377, 2018.

[40] Wong, E., Schmidt, F., Metzen, J. H., and Kolter, J. Z. Scaling provable adversarial defenses. In *Advances in Neural Information Processing Systems*, pp. 8400–8409, 2018.

[41] Xiao, H., Rasul, K., and Vollgraf, R. Fashion-mnist: a novel image dataset for benchmarking machine learning algorithms. 2017.

[42] Zhao, Y., Gao, X., Mullins, R., and Xu, C. Mayo: A framework for auto-generating hardware friendly deep neural networks. 2018.

[43] Zhao, Y., Shumailov, I., Mullins, R., and Anderson, R. To compress or not to compress: Understanding the interactions between adversarial attacks and neural network compression. *arXiv preprint arXiv:1810.00208*, 2018.